

Matrix Metalloproteinase-9 Contributes to Choroidal Neovascularization

Vincent Lambert,* Carine Munaut,* Maud Jost,*
Agnès Noël,* Zena Werb,† Jean-Michel Foidart,*
and Jean-Marie Rakic‡

From the Laboratory of Tumor and Development Biology,*
University of Liège, Liège, Belgium; the Department of Anatomy,†
University of California at San Francisco, San Francisco,
California; and the Department of Ophthalmology,‡ University
Hospital, Sart-Tilman, Liège, Belgium

Age-related macular degeneration (AMD) is the primary cause of irreversible photoreceptors loss in adult patients and current therapies are limited. Increased levels of matrix metalloproteinases (MMPs) have been documented in neovascularization of severe ocular pathologies such as AMD and proliferative diabetic retinopathy. We report here that MMP-9 (gelatinase B) expression is induced and temporally regulated in the course of experimental choroidal neovascularization. We used transgenic mice expressing β -galactosidase reporter gene under the dependence of MMP-9 promoter and RT-PCR analysis on choroidal neovascular structures microdissected from serial sections by laser pressure catapulting to show that MMP-9 expression is up-regulated concomitantly with the appearance of inflammatory cells in the subretinal lesion. In mice deficient in MMP-9 expression the development of choroidal neovascularization induced by laser photocoagulation still occurred, but at a reduced level. (*Am J Pathol* 2002, 161:1247–1253)

Pathological angiogenesis is characteristic of several disease processes affecting the retina, such as retinopathy of prematurity, diabetic retinopathy and the exudative form of age-related macular degeneration (AMD). While the primary stimulus for the development of retinal neovascularization is hypoxia, molecular signals involved in the appearance and growth of pathological choroidal neovascularization are not well defined.¹ While vascular endothelial growth factor (VEGF) overexpression is necessary, alone it is not able to induce growth of choroidal vessels in the subretinal space through the anatomical barrier represented by the intact Bruch's membrane.²

Neovascularization is the result of altered balance between positive and negative regulators of endothelial activation, which leads in turn to basement membrane degradation, endothelial cell migration and proliferation followed by capillary tube formation.³ Such migratory and

tissue remodeling events are regulated by proteolysis mediated by matrix metalloproteinases (MMPs) and serine proteases of the plasminogen/plasminogen activator system. The activities of the secreted MMPs are tightly regulated at multiple levels. These include regulation of gene expression at the level of transcription, secretion of inactive proenzymes, capacity of the active enzyme to be either inhibited by members of the TIMP (tissue inhibitor of metalloproteases) family, or activated by membrane-type MMPs (MT-MMPs). As a rule, basal levels of MMPs are absent or weakly positive in normal tissues, but increase in response to angiogenic cytokines as do the components of the plasminogen/plasminogen activator system.^{4,9}

The precise roles of specific MMPs, plasminogen activators, and their inhibitors in ocular pathology are still being elucidated. Mutations in the TIMP-3 gene give rise to a rare familial form of macular dystrophy associated with subretinal neovascularization.⁵ TIMP-3 is expressed in human retinal pigment epithelium (RPE), and its accumulation is associated with age-related changes in the retina in macular degeneration.^{6,7} The expression of plasminogen activator inhibitor type I (PAI-1) is necessary for the development of choroidal neovascularization in a laser-induced model.⁸

MMP-2 and MMP-9 (gelatinases A and B) are of particular interest because their substrate specificity includes type IV collagen, which must be degraded to facilitate the migration of vascular endothelial cells. These two MMPs show increased expression in a variety of tumors or pathological settings.⁹ Genetic studies in mice indicate that they are required during angiogenesis. MMP-2 is implicated in angiogenic switching in subcutaneous transplants models of tumor progression,¹⁰ whereas MMP-9 is specifically required in a murine model of pancreatic β -cell carcinogenesis.¹¹ MMPs effects are far from being restricted to extracellular matrix (ECM) degradation (reviewed in ref. 12). Peptide growth

Supported by grants from Les Amis des Aveugles, Ghlin, the Fondation Léon Frédéricq, University of Liège, the Fonds d'Investissements de Recherche Scientifique, CHU, Liège, the CGER-Assurances, Belgium, and the Steinbach Fund, New York. C.M. is a research associate and A.N. is a senior research associate from the National Fund for Scientific Research, Belgium.

V.L. and C.M. contributed equally to this work.

Accepted for publication June 21, 2002.

Address reprint requests to Vincent Lambert, Laboratory of Tumor and Development Biology, Pathology Tower (B23), Sart-Tilman, B-4000 Liège, Belgium. E-mail: vincent.lambert@ulg.ac.be.

factors that are sequestered by ECM proteins become available once degraded by MMP-9.¹³ MMPs can increase the bioavailability of VEGF¹¹ but also generate angiogenesis inhibitors such as angiostatin by cleavage of plasminogen.¹⁴ In the eye, high levels of MMP-9 and MMP-2 have been measured in human diabetic vitreous fluids or in epiretinal membranes surgically removed in case of proliferative diabetic retinopathy.^{15–17} Choroidal neovascular membranes surgically removed from patients suffering from AMD also show strong expression of these MMPs, suggesting that they could cooperate in the progression of choroidal angiogenesis.¹⁸

In this study we have characterized the temporal and spatial pattern of MMP-9 expression in a mouse laser-induced model of choroidal neovascularization using three different approaches: immunohistochemistry, transgenic mice expressing β -galactosidase reporter gene under the dependence of MMP-9 promoter, and RT-PCR analysis on choroidal neovascular structures microdissected by laser pressure catapulting. To characterize the relative contribution of MMP-9 to the development of choroidal angiogenesis, we compared subretinal neovascularization in MMP-9-deficient mice and in wild-type (WT) controls.

Materials and Methods

Genetically Modified Mice (*LacZ* Transgene and MMP-9-Deficient)

Construction of mouse line 7700ExIn-LacZ, which contains 7.7 kb of the 5'-flanking region and the first exon and intron of the MMP-9 gene linked to a β -galactosidase gene, was previously described.¹⁹ Promoter activity in this transgenic line closely parallels the activity of the endogenous MMP-9 gene during embryonic development. Homozygous 7700ExIn-LacZ mice for the transgene were mated together to generate new progeny. Expression of the transgene was determined in 2% paraformaldehyde –0.2% glutaraldehyde fixed tissues (15 to 30 minutes), washed three times in PBS, and stained with buffered 5-bromo-4-chloro-3-indolyl- β -galactopyranoside (X-Gal) solution as described.²⁰ As a positive control for MMP-9 expression, a thermal injury was applied to a few mice corneas.²¹ We used the progeny of heterozygous breeding pairs of mice with targeted disruption of MMP-9, as described by Vu et al.²² Brothers and sisters from the same litter were used and genotyped by RT-PCR.²³ Homozygous MMP-9-deficient mice (MMP-9^{-/-}) and the corresponding WT mice (MMP-9^{+/+}) of either sex²² were used in experiments in which neovascular membranes were quantified. All of the animals used in this study were maintained with a 12-hour light/12-hour dark cycle and had free access to food and water.

Murine Model of Laser-Induced Choroidal Neovascularization

Animal experiments were performed in compliance with the Association for Research in Vision and Ophthalmol-

ogy (ARVO) statement for the Use of Animals in Ophthalmic and Vision Research. Choroidal neovascularization was induced in mice by four burns (usually at the 6, 9, 12, and 3 o'clock positions around the optic disk) using a green argon laser (532 nm; 50 μ m diameter spot size; 0.05 seconds duration; 400 mW) as previously described.²⁴ Animals (five or more in each group) were sacrificed at day 2, 3, 5, 10, 14, and 28 for the evaluation of the kinetic of MMP-9 expression, and at day 14 in the experiment involving MMP-9^{-/-} and WT mice comparison. In the latter group, before sacrifice, fluorescein angiograms (intraperitoneal injection of 0.3 ml of 1% fluorescein sodium; Ciba) were performed to evaluate the percentage of laser burns developing late phase hyperfluorescent spots (corresponding to the leakage of fluorescein from newly formed permeable capillaries). The eyes were then enucleated and either fixed in buffered 3.5% formalin solution for routine histology or embedded in TissueTeK (Miles Laboratories, Naperville, IL) and frozen in liquid nitrogen for cryostat sectioning. Choroidal neovascularization was quantified as previously described.⁸ Briefly, frozen serial sections were cut throughout the entire extent of each burn, and the thickest lesions (minimum of 3/lesion) used for the quantification. Using a computer-assisted image analysis system (Olympus Micro Image version 3.0 for Windows 95/NT, Olympus Optical Co. Europe GmbH), neovascularization was estimated by the ratio (B/C) of the thickness from the bottom of the pigmented choroidal layer to the top of the neovascular membrane (B) to the thickness of the intact-pigmented choroid adjacent to the lesion (C). Due to the small size of most lesions, that method was preferred to surface estimation for its independence in relation to oblique sections, its reproducibility and correlation with fluorescein angiograms results.

Immunohistochemistry

Cryostat sections (5 μ m thick) were fixed in paraformaldehyde 1% in 0.07 mol/L phosphate-buffered saline (PBS) pH 7.0 for 5 minutes or in acetone for 10 minutes at room temperature and then incubated with the primary antibody. Antibodies raised against type IV collagen (guinea pig polyclonal antibody produced in our laboratory; diluted 1/100), mouse MAC-1 (monoclonal antibody anti CD-11b R-phycoerythrin labeled, PharMingen, San Diego, CA; diluted 50 μ g/ml), mouse neutrophils (rat polyclonal antibody, Serotec, Oxford, UK; diluted 1/200) and mouse PECAM (rat monoclonal antibody, PharMingen, San Diego, CA; diluted 1/20) were incubated for 1 hour at room temperature, whereas antibodies to MMP-9 (rabbit anti-mouse antibody, diluted 1/200, a generous gift from P. Carmeliet, Katholieke Universiteit Leuven, Belgium) were incubated overnight. The sections were washed in PBS (3 \times 10 minutes) and appropriate secondary antibodies conjugated to fluorescein-isothiocyanate (FITC) or Texas red were added: swine anti-rabbit IgG (Dako, Glostrup, Denmark; diluted 1/40), monoclonal anti-guinea pig IgG (Sigma; diluted 1/40) or rabbit anti-rat IgG (Sigma; diluted 1/40) were applied for 30 minutes.

For double immunofluorescence-labeling studies, sections were first incubated with the two primary antibodies, and then with FITC- and Texas red-conjugated secondary antibodies. After three washes in PBS for 10 minutes each and a final rinse in 10 mmol/L Tris-HCl buffer, pH 8.8, labeling was analyzed under an inverted microscope equipped with epifluorescence optics. MAC-1 and neutrophils sections were counterstained with bis-benzimide (20 mg/100 ml) for 15 minutes. Specificity of staining was assessed by substitution of nonimmune serum for primary antibody (in the case of MMP-9 protein, MMP-9^{-/-} tissues were used as a negative control).

Laser Pressure Catapulting (LPC) and RT-PCR

Eight to 10 serial frozen sections were mounted directly onto a 1.35- μ m thin polyethylene foil (PALM, Wolfrahtshausen, Germany). The supporting membrane was mounted onto the glass slide using the Microbeam-MO-MeNT technique.²⁵ The membrane-covered slides can be stored at room temperature until needed. The Robot-Microbeam (PALM) focused the laser (337 nm) on the specimen with appropriate energy settings enabling the catapulting of the entire selected area into the Microfuge cap. The entire subretinal choroidal neovascularization area and an adjacent intact chorioretinal zone (control) were microdissected separately on frozen sections (10 μ m thick) at selected intervals after laser burn (days 3, 5, 10, 14, and 40). The specimens were covered with 100 μ l of lysis buffer and total RNA isolation was performed with the PUREscript RNA-isolation Kit (BIOzym, Landgraaf, The Netherlands) according to the manufacturer's protocol. Total RNA was dissolved in a 10- μ l RNA hydration solution supplied by the manufacturer. 28S rRNA were amplified with an aliquot of 1 μ l of total RNA using the GeneAmp Thermo-stable rTth reverse transcriptase RNA PCR kit (Perkin Elmer) and three pairs of primers (Gibco BRL-Life Technologies): sense: 5'-GTTCAACCCACTAATAGGGAACGTGA-3' and reverse: 5'-GGATTCTGACTTAGAGGCGTTCAGT-3' for 28S mRNA; sense: 5'-AGACCTGAAAACCTCCAACCTCAC-3' and reverse: 5'-TGTTATGATGGTCCCACCTTGAGGC-3' for MMP-9; and sense: 5'-AGATCTTCTTCTCAAGGACCG-GTT-3' and reverse: 5'-GGCTGGTCAGTGGCTT-GGGGTA-3' for MMP-2. Reverse transcription was performed at 70°C for 15 minutes followed by 2 minutes of incubation at 95°C for denaturation of RNA-DNA heteroduplexes. Amplification started by 15 seconds at 94°C, 20 seconds at 68°C and 10 seconds at 72°C for MMP-2 and 28S (45 cycles for MMP-2 and 30 cycles for 28S) or by 15 seconds at 94°C, 20 seconds at 60°C, and 15 seconds at 72°C for MMP-9 (45 cycles) and terminated by 2 minutes at 72°C. RT-PCR products were resolved on 2% agarose gels and analyzed using a Fluor-S Multimager (BioRad) after staining with GelStar (FMC BioProducts) dye. The expected size for RT-PCR products were 212 bp for 28S, 225 bp for MMP-2, and 262 bp for MMP-9, respectively.

Gelatin Zymography Assay

Choroidal neovascularization was induced in mice by 30 burns as described above. Animals were sacrificed at

day 3 and the eyes were enucleated. The posterior segments were cut out and immediately snap frozen in liquid nitrogen. Frozen tissues were then pulverized in liquid nitrogen, homogenized in buffer (0.1 mol/L Tris-HCl pH 8.1, 0.4% Triton X-100) and centrifuged for 20 minutes at 5000 \times g. The pellets were discarded. Aliquots of supernatants were mixed with SDS sample buffer and electrophoresed directly as previously described.²⁶

Statistical Analysis

Data were analyzed with GraphPad Prism 3.0 (San Diego, CA). The Mann-Whitney test was used to determine whether there were significant ($P < 0.05$) differences between WT and MMP-9^{-/-} mice.

Results

MMP-9 Induction and Evolution

The argon laser induced trauma at the level of outer retina, retinal pigment epithelium and Bruch's membrane, giving rise to choroidal neovascularization under the retina, similar to that observed in exudative form of AMD. Histological analysis and immunostaining with anti-PECAM and anti-collagen type IV antibodies confirmed the presence of newly formed capillaries taking typically the form of "mushroom-like" areas (identifiable already at day 5) over the normal choroid layer.

Immunohistochemical staining demonstrated the presence of MMP-9 protein exclusively at the site of laser-induced injury (retinal pigment epithelium and choroidal layer) and not in intact adjacent areas (Figure 1A). The intensity of staining was maximal at day 3 (before any visible outgrowth of newly formed microvessels), weak at day 5 (Figure 1B) and completely absent thereafter. No staining was observed at any location in MMP-9^{-/-} mice (not shown). The staining in the positive control (thermal injury of the cornea) was also maximal at day 3 and present selectively in the corneal stroma adjacent to the burned area (Figure 1C) as previously described.²⁷

MMP-9 promoter activity, mapped with β -galactosidase reporter gene, was undetectable in the retina or in the cornea of intact eyes. In treated eyes, it did not strictly colocalize either spatially or temporally with MMP-9 protein. The product of the β -galactosidase reaction could not be detected before day 5 (Figure 1D) both in the chorioretinal neovascular membrane (Figure 1E) and in the corneal epithelium (positive control, Figure 1F). It was only occasionally detected after day 5. The product of the β -galactosidase reporter gene was localized at the growing edge of the neovascular reaction over the plane of the pigment epithelium. The activity of MMP-9 promoter in the lesions at day 5 coincided with the first appearance of macrophages detected by immunohistochemistry (Figure 2, A–D). Polymorphonuclear cells were absent at day 5 but infiltrated the lesions at an earlier stage (Figure 2, E and F).

RT-PCR analysis applied on microdissected neovascular choroidal membranes extracted by laser pressure

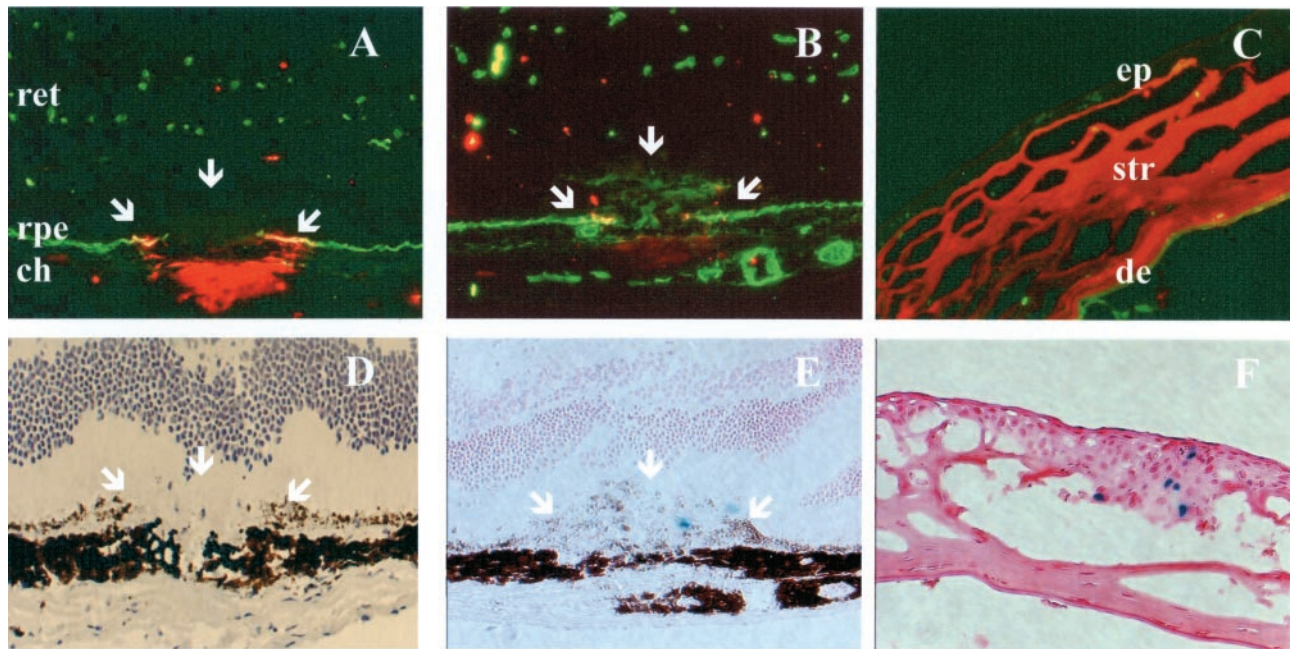


Figure 1. Temporal pattern of protein and MMP-9 mRNA presence after laser-induced choroidal neovascularization. **A–C:** Immunolocalization of MMP-9 (red) in ocular frozen sections counterstained with collagen type IV antibody (green) at day 3 (**A**), day 5 (**B**) after laser injury of the Bruch's membrane, and in corneas subjected to thermal injury (**C**) (positive control). **D–F:** Mapping of MMP-9 expression using transgene mice expressing β -galactosidase (blue) under the dependence of MMP-9 promoter at day 3 (**D**) and day 5 (**E**) in the retina and at day 5 in the cornea (**F**). **White arrows** localize the laser impact. The neural retina (ret), retinal pigment epithelium (rpe), choroidal layer (ch), corneal epithelium (ep), corneal stroma (str) and descemet membrane (de) are indicated. Original magnification, $\times 100$.

catapulting at different time endpoints confirmed MMP-9 mRNA expression only at day 5 after photocoagulation, similarly to the results obtained with the β -galactosidase transgene (Figure 3). The retinal specimens microdissected from neighboring intact chorioretinal areas were negative for MMP-9 mRNA throughout the study period. This contrasted with the expression of MMP-2, which was relatively constant from day 3 to day 14 with a small peak at day 10 (Figure 3, center line). Unlike MMP-9, MMP-2 expression was not restricted to the choroidal neovascular area and was also detected, at a lower level, outside the impact zone in intact chorioretinal tissue.

The activities of MMP-2 and MMP-9 posterior eyes segments of normal mice and in neovascular choroidal membranes induced by laser were analyzed by gelatin zymography. The latent form of MMP-2 was detected in all tissue extracts (Figure 4). Its level was however more

important in laser induced membranes which additionally contained active MMP-2. MMP-9 activity was weakly detected in intact eyes, whereas higher levels were found in laser treated eyes.

Choroidal Neovascularization in Vivo in MMP-9^{-/-} and WT Mice

To determine whether the absence of MMP-9 influences choroidal neovascularization *in vivo*, we first evaluated the incidence of leaking spots on fluorescein angiograms performed on day 14. Newly formed microvessels with significant leakage of fluorescein were observed in 75% of the laser-induced lesions. The incidence of detected leaking spots was not significantly different in MMP-9^{-/-} mice compared to their WT controls (not shown). Neo-

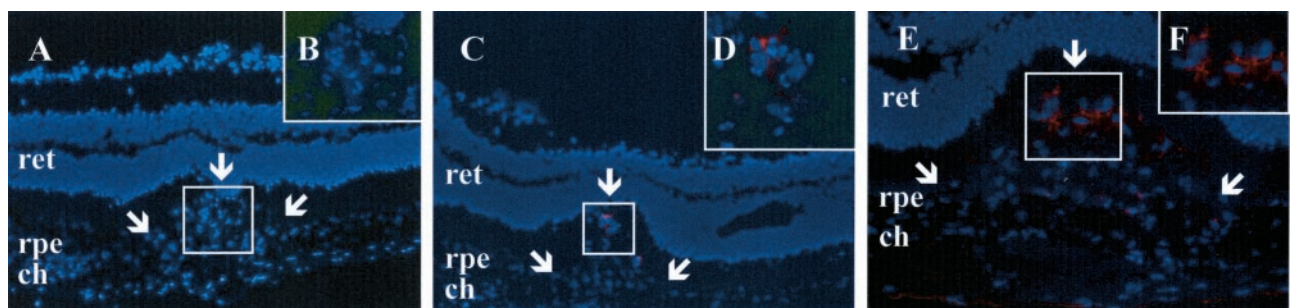


Figure 2. Immunolocalization of mononuclear and polymorphonuclear inflammatory cells during the course of choroidal neovascular membrane development after laser injury of the choroid. Mac-1 immunostaining (red) on frozen sections counterstained with bis-benzimide (blue) is absent in the choroid at day 3 (**A**, **B**), and appears in the impact at day 5 (**C**, **D**). Neutrophils (red) are present at day 3 (**E**, **F**), but not at day 5 (data not shown). **White arrows** localize the laser impact. Original magnifications: **A**, **C**, $\times 100$; **B**, **D**, **E**, $\times 400$; **F**, $\times 630$.

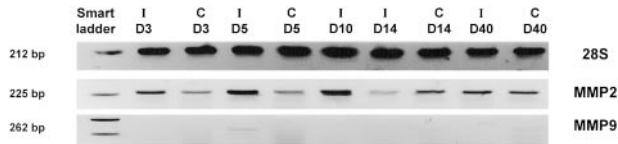


Figure 3. MMP-2 and MMP-9 expression are differentially modulated during the progression of choroidal neovascular reaction in a murine laser-induced model. Laser pressure catapulting followed by RT-PCR analysis on microdissected choroidal new vessels (I) and on adjacent (control) intact chorioretinal tissue (C) from day 3 to day 40. Molecular weight numbers (bp) are shown at left. The control at day 10 is missing due to limited amount of extracted RNA.

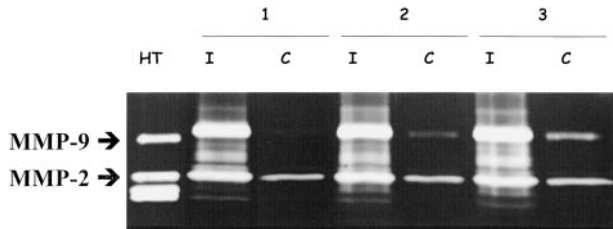


Figure 4. Zymographic analysis of MMP-2 and MMP-9 in tissues extracted either from posterior eyes segments with laser-induced neovascularization (I, day 3) or intact eyes (C) of three different mice. As positive control, medium conditioned by human HT1080 cells was included. Positions of MMP-2 and MMP-9 are indicated by arrows.

vascularization was then estimated by immunostaining with anti-type IV collagen and anti-PECAM antibodies and, histologically, by measuring, on serial sections, the maximal height of the lesion above the choroidal layer observed in neighboring intact zones (Figure 5). Choroidal neovascularization at the site of laser-induced trauma was more restricted reaction in MMP-9^{-/-} mice than in WT mice. This was quantified by determining the B/C ratio between total thickness of lesions (B, from the bottom of the choroid to the top of the neovascular area) to the thickness of adjacent normal choroid (C), and a 20% reduction of the B/C ratio was consistently observed in MMP-9-deficient mice ($P < 0.001$) as compared to WT mice (Figure 6).

Discussion

The matrix metalloproteinases (MMPs) are able to degrade components of the extracellular matrix, inhibitors, and other pericellular proteins and promote angiogenesis and tumor invasion. MMP-2 and MMP-9 have been of particular interest in angiogenesis research because

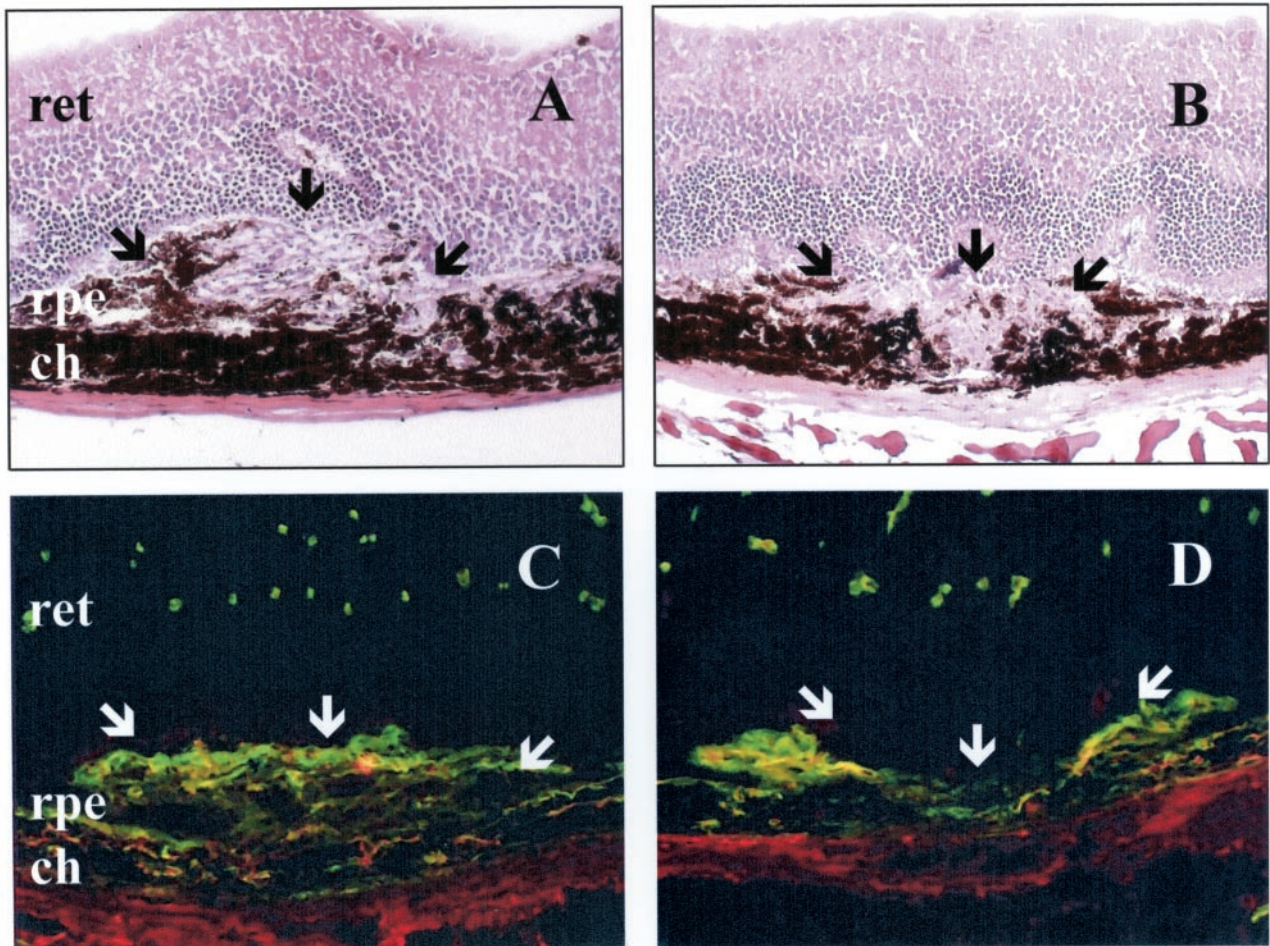


Figure 5. Histological analysis after laser treatment. Hematoxylin-eosin staining of a representative area of choroidal neovascularization at the site of laser-induced trauma in WT mice (A), and a more restricted reaction in MMP-9^{-/-} mice (B). Immunofluorescence labeling of new vessels in WT (C) or in MMP-9^{-/-} mice (D) analyzed 14 days after laser photocoagulation. New vessels were detected with anti-mouse anti-collagen type IV antibody (green) and anti-mouse anti-PECAM antibody (red). The neural retina (ret), retinal pigment epithelium (rpe), and choroidal layer (ch) are indicated and the neovascular area is arrowed. White arrows localize the laser impact. Original magnification, $\times 200$

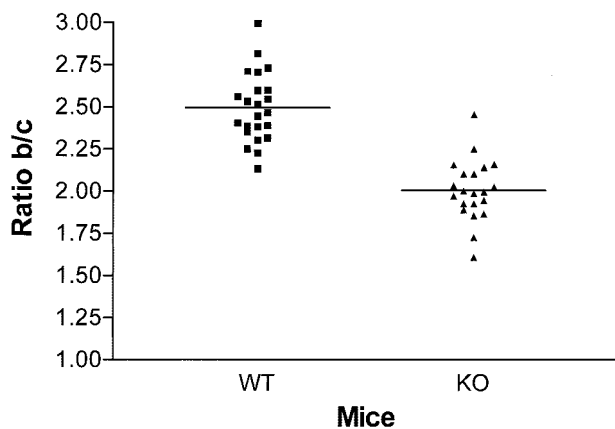


Figure 6. Reduced neovascularization in MMP-9^{-/-} mice. Angiogenesis was quantified by evaluating the B/C ratio as described previously⁸ at day 14 after laser injury of the Bruch's membrane. Results are shown as column scatter; $P < 0.001$ (unpaired, non-parametric Mann-Whitney).

their substrate specificity includes type IV collagen, a major component of basement membranes and of the subretinal Bruch's membrane. However, MMP action can be both proangiogenic and antiangiogenic. While MMP-9 regulates the bioavailability of VEGF,¹¹ stimulating angiogenesis, MMPs also generate antiangiogenic factors and degrade basement membranes, which may destabilize the newly formed blood vessels, thus trimming back and limiting the extent of angiogenesis.²⁸

Since MMP-9 expression has been demonstrated in human proliferative ischemic chorioretinopathies²⁹ and in experimental ocular models,³⁰ the aim of our investigation was to determine whether MMP-9 plays a role in laser-induced choroidal neovascularization, a model similar to the exudative AMD, the most sight-devastating form of human AMD.

MMP-9 mRNA expression was mapped using transgenic mice expressing β -galactosidase reporter gene under the dependence of MMP-9 promoter. RT-PCR analysis was performed on choroidal neovascular structures microdissected from serial sections by laser pressure catapulting. To our knowledge, this is the first report applying microdissection techniques to study gene expression in experimental subretinal neovascularization. These two approaches cooperatively demonstrated that the local expression of MMP-9 mRNA is restricted to day 5 after laser burn. Although resident cells might also produce MMP-9, mRNA detection coincides perfectly with the appearance of macrophages within the neovascular reaction. This suggests that inflammatory cells are a predominant provider of MMP-9, as found previously in tumor models.³¹ Indeed, an angiogenic role for macrophages infiltrating choroidal new vessels has already been reported.³² A previous study using krypton laser in rats to induce choroidal neovascularization did not find a change in the expression of MMP-9 using *in situ* hybridization.³³ Differences in methodology, animal model and sensitivity of the techniques and the very narrow time window of expression probably explain these apparent discrepancies.

It is worth noting that inflammatory cells containing preformed MMP-9 in intracellular granules could also contribute to the development of the lesions. Since the contribution of these providers of MMP-9 protein would not be detected by the MMP-9 evaluation at the mRNA levels, it was therefore important to compare protein and mRNA expressions. At the protein level, MMP-9 activity was observed with zymography and was immunohistochemically localized in the laser-induced lesion already at day 3, before local mRNA expression was detected. Thus MMP-9 probably first arose from early recruitment and degranulation of neutrophils before a transcriptional induction of its local expression and that preformed protein might represent the major source of active MMP-9.

The pattern of MMP-2 expression obtained by RT-PCR on microdissected samples is different from that of MMP-9. MMP-2 was constantly expressed throughout the study period both in the choroidal neovascular membrane and in control adjacent intact areas, with a relative peak of expression at day 10 whose significance is at present unclear. These data confirm the clear different regulation pattern of MMP-2 and MMP-9.

MMP-9 Contributes to Choroidal Neovascularization in the Murine Laser-Induced Model

Angiogenesis determined by immunohistochemistry and quantitative histology was significantly reduced in MMP-9-deficient animals compared to WT controls. The pattern of MMP-2 expression demonstrated that MMP-2 did not compensate for the deficiency of MMP-9. Our results provide for the first time evidence that MMP-9 contributes to choroidal neovascularization induced by laser although they do not distinguish whether MMP-9 exerts its role directly or through the release and/or activation of other angiogenic factors such as VEGF.^{11,34} However, the magnitude of angiogenesis inhibition was much less important than that observed previously in the same model applied on mice deficient for plasminogen activator type 1.⁹ This in turn suggests that MMP-9 is not the only pathway for rendering angiogenic factors bioavailable, which clearly occurs for VEGF-dependent angiogenesis later in tumor progression.¹¹ Nevertheless the MMP-9 induction restricted to day 5 after laser-induced rupture of the Bruch's membrane contributed to the severity of pathological choroidal neovascularization. Taken together with the previous work on PAI-1, these data indicate that a balance of both positive and negative regulation of proteolysis by more than one enzyme system are critical to overall neoangiogenesis. One implication of our observations is that combination of MMP-9 inhibitors with other anti-angiogenic agents may be a promising strategy.

References

1. Campochiaro PA: Retinal and choroidal neovascularization. *J Cell Physiol* 2000, 184:301-310

2. Schwesinger C, Yee C, Rohan RM, Jousen AM, Fernandez A, Meyer TN, Poulaki V, Ma JJK, Redmond TM, Liu S, Adamis AP, D'Amato RJ: Intrachoroidal neovascularization in transgenic mice overexpressing vascular endothelial growth factor in the retinal pigment epithelium. *Am J Pathol* 2001, 158:1161-1172
3. Hanahan D, Folkman J: Patterns and emerging mechanisms of the angiogenic switch during tumorigenesis. *Cell* 1996, 86:353-364
4. Mandriota SJ, Pepper MS: Vascular endothelial growth factor-induced in vitro angiogenesis and plasminogen activator expression are dependent on endogenous basic fibroblast growth factor. *J Cell Sci* 1997, 110:2293-2302
5. Weber B, Vogt G, Pruetz RC, Stohr H, Felbor U: Mutations in the tissue inhibitor of metalloproteinases-3 (TIMP3) in patients with Sorsby's fundus dystrophy. *Nat Genet* 1994, 8:352-356
6. Ruiz A, Brett P, Bok D: TIMP-3 is expressed in the human retinal pigment epithelium. *Biochem Biophys Res Commun* 1996, 226:467-74
7. Kamei M, Hollyfield JG: TIMP-3 in Bruch's membrane: changes during aging and in age-related macular degeneration. *Invest Ophthalmol Vis Sci* 1999, 40:2367-2375
8. Lambert V, Munaut C, Noel A, Frankenne F, Bajou K, Gerard B, Carmeliet P, Defresne MP, Foidart J-M, Rakic J-M: Influence of plasminogen activator inhibitor type I on choroidal neovascularization. *FASEB J* 2001, 15:1021-1027
9. Pepper MS: Role of the matrix metalloproteinase and plasminogen activator-plasmin systems in angiogenesis. *Arterioscler Thromb Vasc Biol* 2001, 21:1104-1117
10. Itoh T, Tanioka M, Yoshida H, Yoshioka T, Nishimoto H, Itohara S: Reduced angiogenesis and tumor progression in gelatinase A-deficient mice. *Cancer Res* 1998, 58:1048-1051
11. Bergers G, Brekken R, McMahon G, Vu TH, Itoh T, Tamaki K, Tanzawa K, Thorpe P, Itohara S, Werb Z, Hanahan D: Matrix metalloproteinase-9 triggers the angiogenic switch during carcinogenesis. *Nat Cell Biol* 2000, 2:737-744
12. Chang C, Werb D: The many faces of metalloproteinases: cell growth, invasion, angiogenesis, and metastasis. *Trends Cell Biol* 2001, 11:S37-S43
13. Manes S, Llorente M, Lacalle RA, Gomez-Mouton C, Kremer L, Mira E, Martinez-AC: The matrix metalloproteinase-9 regulates the insulin-like growth factor-triggered autocrine response in DU-145 carcinoma cells. *J Biol Chem* 1999, 274:6935-6945
14. Dong Z, Kumar R, Yang X, Fidler IJ: Macrophage-derived metalloelastase is responsible for the generation of angiostatin in Lewis lung carcinoma. *Cell* 1997, 88:801-810
15. Das A, McGuire PG, Eriqat C, Ober RR, DeJuan Jr E, Williams GA, McLamore A, Biswas J, Johnson DW: Human diabetic neovascular membranes contain high levels of urokinase and metalloproteinase enzymes. *Invest Ophthalmol Vis Sci* 1999, 40:809-813
16. Kosano H, Okano T, Katsura Y, Noritake M, Kado S, Matsuoka T, Nishigori H: ProMMP-9 (92 kDa gelatinase) in vitreous fluid of patients with proliferative diabetic retinopathy. *Life Sci* 1999, 64:2307-2315
17. Jin M, Kashiwagi K, Iizuka Y, Tanaka Y, Imai M, Tsukahara S: Matrix metalloproteinases in human diabetic and nondiabetic vitreous. *Retina* 2001, 21:28-33
18. Steen B, Sejersen S, Berglin L, Seregard S, Kvanta A: Matrix metalloproteinases and metalloproteinase inhibitors in choroidal neovascular membranes. *Invest Ophthalmol Vis Sci* 1998, 39:2194-2200
19. Munaut C, Salonurmi T, Kontusaari S, Reponen P, Morita T, Foidart JM, Tryggvason K: Murine matrix metalloproteinase 9 gene 5'-upstream region contains cis-acting elements for expression in osteoclasts and migrating keratinocytes in transgenic mice. *J Biol Chem* 1999, 274:5588-5596
20. Behringer RR, Crotty DA, Tennyson VM, Brinster RL, Palmiter RD, Wolgemuth DJ: Sequences 5' of the homeobox of the Hox-1.4 gene direct tissue-specific expression of lacZ during mouse development. *Development* 1993, 117:823-833
21. Mohan R, Rinehart WB, Bargagna-Mohan P, Fini E: Gelatinase B/lacZ transgenic mice, a model for mapping gelatinase B expression during developmental and injury-related tissue remodeling. *J Biol Chem* 1998, 273:25903-25914
22. Vu TH, Shipley JM, Bergers G, Berger JE, Helms JA, Hanahan D, Shapiro SD, Senior RM, Werb Z: MMP-9/gelatinase B is a key regulator of growth plate angiogenesis and apoptosis of hypertrophic chondrocytes. *Cell* 1998, 93:411-422
23. Ducharme A, Frantz S, Aikawa M, Rabkin E, Lindsey M, Rohde LE, Schoen FJ, Kelly RA, Werb Z, Libby P, Lee RT: Targeted deletion of matrix metalloproteinase-9 attenuates left ventricular enlargement and collagen accumulation after experimental myocardial infarction. *J Clin Invest* 2000, 106:55-62
24. Tobe T, Ortega S, Luna JD, Ozaki H, Okamoto N, Derevjank NL, Vinores SA, Basilico C, Campochiaro PA: Targeted disruption of the FGF2 gene does not prevent choroidal neovascularization in a murine model. *Am J Pathol* 1998, 153:1641-1646
25. Bohm M, Wieland I, Schutze K, Rubben H: Microbeam MOMENT: non-contact laser microdissection of membrane-mounted native tissue. *Am J Pathol* 1997, 151:63-67
26. Munaut C, Noel A, Weidle UH, Krell HW, Foidart JM: Modulation of the expression of interstitial and type-IV collagenases in coculture of HT1080 fibrosarcoma cells and fibroblasts. *Invasion Metastasis* 1995, 15:169-178
27. Fini ME, Parks WC, Rinehart WB, Girard MT, Matsubara M, Cook JR, West-Mays JA, Sadow PM, Burgeson RE, Jeffrey JJ, Raizman MB, Krueger RR, Zieske JD: Role of matrix metalloproteinases in failure to re-epithelialize after corneal injury. *Am J Pathol* 1996, 149:1287-1302
28. Yamada E, Tobe T, Yamada H, Okamoto N, Zack DJ, Werb Z, Soloway PD, Campochiaro PA: TIMP-1 promotes VEGF-induced neovascularization in the retina. *Histol Histopathol* 2001, 16:87-97
29. Salzmann J, Limb GA, Khaw PT, Gregor ZJ, Webster L, Chignell AH, Charteris DG: Matrix metalloproteinases and their natural inhibitors in fibrovascular membranes of proliferative diabetic retinopathy. *Br J Ophthalmol* 2000, 84:1091-1096
30. Majka S, McGuire P, Colombo S, Das A: The balance between proteinases and inhibitors in a murine model of proliferative retinopathy. *Invest Ophthalmol Vis Sci* 2001, 42:210-215
31. Coussens LM, Tinkle CL, Hanahan D, Werb Z: MMP-9 supplied by bone marrow-derived cells contributes to skin carcinogenesis. *Cell* 2000, 103:481-490
32. Oh H, Takagi H, Suzuma K, Otani A, Ishida K, Matsumura M, Ogura Y, Honda Y: The potential angiogenic roles of macrophages in the formation of choroidal neovascular membranes. *Invest Ophthalmol Vis Sci* 1999, 40:1891-1898
33. Kvanta A, Shen W-Y, Sarman S, Seregard S, Steen B, Rakoczy E: Matrix metalloproteinase (MMP) expression in experimental choroidal neovascularization. *Curr Eye Res* 2000, 21:684-690
34. Engsig MT, Chen Q-J, Vu TH, Pedersen A-C, Therkidsen B, Lund LR, Henriksen K, Lenhard T, Foged NT, Werb Z, Delaissé J-M: Matrix metalloproteinase 9 and vascular endothelial growth factor are essential for osteoclast recruitment into developing long bones. *J Cell Biol* 2000, 151:879-889